Member Report
China

ESCAP/WMO Typhoon Committee
The 15th Integrated Workshop

1-2 December, 2020

CONTENTS

I. Review of Tropical Cyclones Affecting China since Last Session of ESCAP/WMO Typhoon Committee

1.1 Meteorological and Hydrological Assessment

A weak El Niño event lingered from November 2019 to April 2020 over the tropical central and eastern Pacific. Meanwhile, the warmer northern Indian Ocean water sustained from spring to summer, resulting in extremely intense western Pacific subtropical highs in summer, a distinctly southward position of the subtropical ridge in July, an unusual weakening of the South China Sea monsoon trough, starkly fewer TCs over the NW Pacific for this summer, and even zero TC for last July.

As of 20 October 2020 the NW Pacific and South China Sea witnessed the generation of 17 TCs, 5.3 fewer than the multi-year average for the same period (22.3). Among them, 5 TCs made landfall over coastal China, namely, Nuri (2002), Hagupit (2004), Mekkhala (2006), Higos (2007) and Nangka (2016). This number is 1.7 lower than the multi-year average for the same period (6.7).

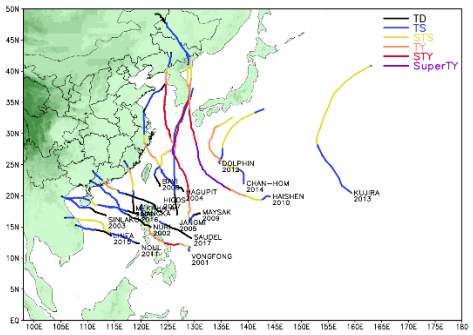

Fig1.1 Tracks of TCs over NW Pacific and South China Sea from 1 January to 20 October 2020

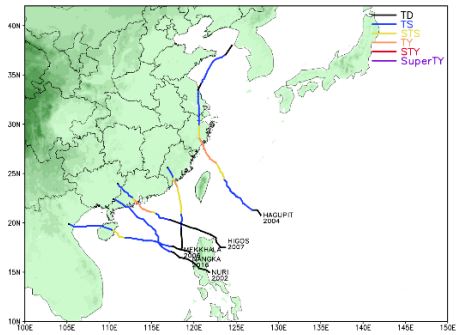

Fig1.2 Tracks of TCs that made landfall over China from 1 January to 20 October 2020

1.1.1 Characteristics of 2020 TCs

This year came up with fewer TCs and landfalling TCs, a distinct shift of the typhoon birthplaces westward, a summer featuring conversion from an "extraordinarily silent" to very active TC season, with NE China visited more than usual.

1) Distinctly Westward TC Genesis Locations

The average genesis location of the 17 TCs occurring this year (as of 20 October) is 18.6°N, 126.3°E. It is 10.2 degrees of longitude farther westward than the multi-year average genesis location (16.1°N, 136.5°E). The farther westward the genesis location is, the more likely the TC is to make landfall in or affect China (Fig 1.4).

2) Fewer TCs and Lower TC Intensity

By 20 October, 17 TCs have occurred over the NW Pacific and the South China Sea, 5.7 lower than the multi-year average for the same period of time. The average peak intensity of these TCs is 33.9 m/s, which is obviously lower than the multi-year average of 40.1 m/s.

3) Fewer Landing TCs with Levelling-Off Landing Intensity

As of 20 October China has been visited by 5 TCs (Nuri, Hagupit, Mekkhala, Higos and Nangka), 1.7 fewer than the multi-year average over the same period of time. The 5 TCs landed with an average intensity of 30.8 m/s, slightly lower than the multi-year average of 32.6 m/s.

4) A New Record of 0 TC for July

No TCs occurred over the NW Pacific and the South China Sea last July, setting a zero TC record for July in the meteorological history since 1949.

5) A TC-Active August Marked by Fast Offshore Intensification

A total of 7 TCs occurred last August, 1.3 more than the multi-year average August number of 5.7 TCs, among which 4 TCs appearing in the first ten days of the month, three landed in China, i.e., Hagupit, Mekkhala,

and Higos. This number is 1.1 higher than the multi-year average of 1.9. And, they all underwent fast offshore intensification to land with peak intensity. It is worth noting that Mekkhala landed 20.5 hours after its formation over the South China Sea, less than a half of the average of other "local" TCs (48.6 hours). Such a short interval posed a big challenge to TC forecasting.

6) NE China Hit by Three TCs in Succession - Rare in History

NE China was hit in quick succession by three typhoons - Bavi, Maysak and Haishen - from 26 August to 8 September, being unprecedented in local meteorological history and outnumbering the normal-year record of (1.2) TCs affecting NE China by additional 1.8.

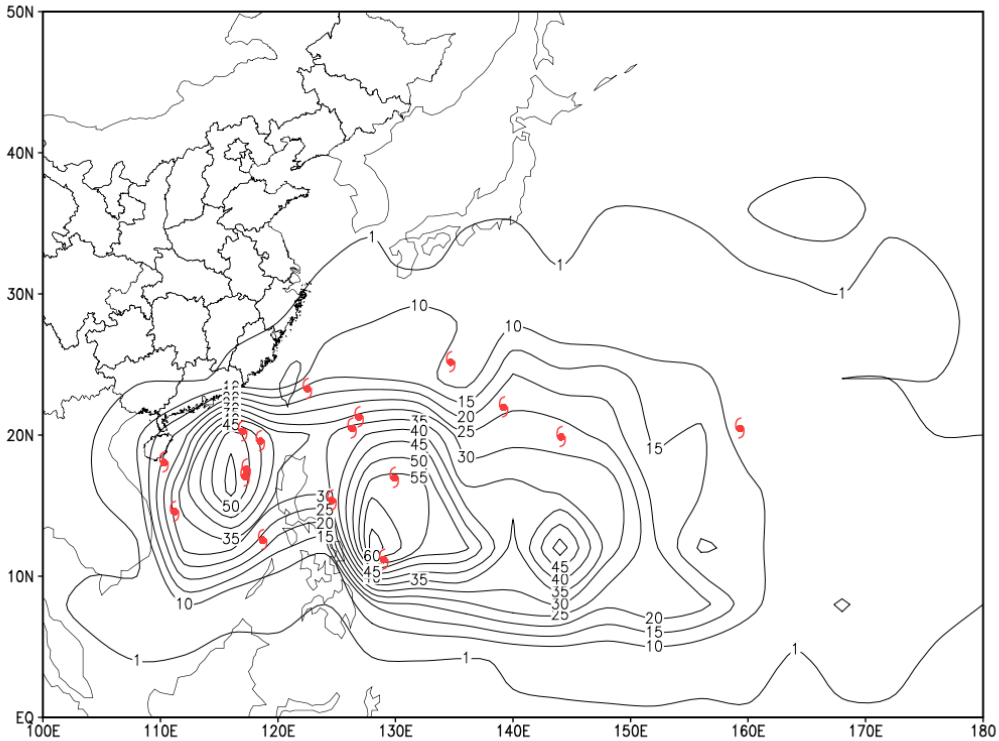

Fig 1.3 1949-2019 NW Pacific and South China Sea tropical cyclone source region density distribution (Resolution: 2.5°×2.5°) and genesis location of tropical cyclones forming from 1 January to 20 October 2020

1.1.2 Precipitation of TCs Affecting China

Since the beginning of 2020, 17 TCs have emerged over the NW Pacific and the South China Sea, 5 of which made landfall over China. Of the 5 TCs, 3 landed along western Guangdong to southern Fujian, 1 at Zhejiang and 1 at Hainan; 3 affected NE China, a record high since 1949. Rainfall is of two main characteristics:

1) Many North-Moving TCs with High Total Precipitation

From late August to early September NE China was afflicted in turn by three TCs - Bavi, Maysak and Haishen, breaking the record since 1949. Under their impact, the maximum accumulated rainfall from 26 August to 9 September over the Songhua and Liao River basins reached 167mm, 3.3 times more than the normal-year figure for the same period and the highest since 1949. Songhua and Liao Rivers marked a respective maximum accumulated rainfall of 182mm and 121mm, or 3.8 and 1.9 times higher more than the normal-year figure for the same period, both being the highest since 1949.

2）Many Rivers Rising above Warning Levels and Some Record Levels

Typhoon precipitation caused water to rise above warning levels for altogether 106 rivers in Zhejiang, Liaoning, Jilin and Heilongjiang provinces. Among them, the Songhua River reported basin-wide flooding; 21 rivers including the Zhaoyuan and Fujin sections of the Songhua River hit their highest safety levels; 5 rivers including the Songhua tributary Chalin, the Hulan tributary Tongken and the Mudan tributary Hengdaohezi broke their record high levels; Chaoyang River, tributary of Buerhatong River, was visited by its biggest flood in 100 years.

1.1.3 TCs Affecting China

1) Tropical Storm Nuri (2002)

Nuri formed as a tropical disturbance offshore eastern Philippines,

strengthening then into a tropical depression at 1200 UTC on 11 June before moving northwestward as Tropical Storm Nuri (2002) at 1200 UTC on 12 June. Nuri made landfall over the coastal Hailing Island, Yangjiang City of Guangdong Province around 0050 UTC on 14 June (Scale 9, 23m/s, 990hPa), and moved farther northwestward into Guangxi before weakening into a tropical depression in Yulin City at 0900 UTC. It was ceased to be numbered at 1200 UTC.

Under the influence of Nuri, the 13-15 June accumulated rainfall reached 50 to 80 mm in parts of southwestern Guangdong, central and southern Guangxi, and Hainan Island; 100 to 166mm in local areas of Laibin and Fangchenggang of Guangxi and of Lingao and Danzhou of Hainan. The precipitation resulted in water rises for small and medium-sized rivers in coastal Guangdong, Guangxi and Hainan, yet below their warning levels. Besides, Nuri also brought gusts of 7-9 scales to the Pearl River Delta and the coastal Guangdong, Hainan and southern Guangxi, and gusts up to 32.9m/s (up to scale 12) to Taishan Island, Jiangmen City, Guangdong Province.

Nuri's influence upon South China was positive in general. The precipitation brought by Nuri helped alleviate the moderate to severe meteorological drought in southwest Guangdong, south Guangxi and Hainan Island lasting from the beginning of flood season.

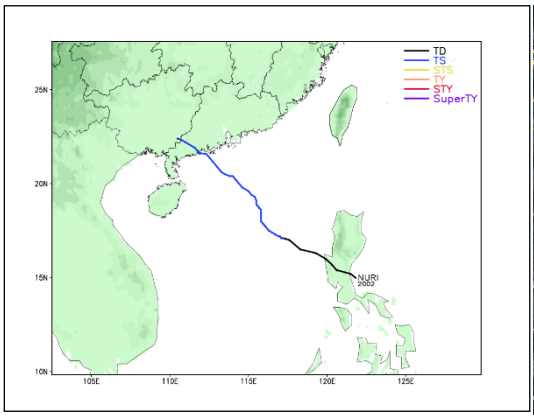

Fig 1.4a Track of Nuri

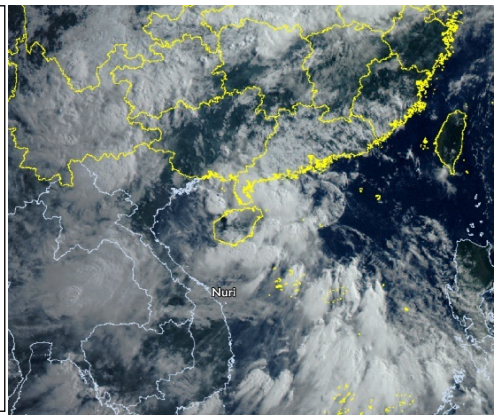

Fig 1.4b FY-4A Satellite Image of Nuri

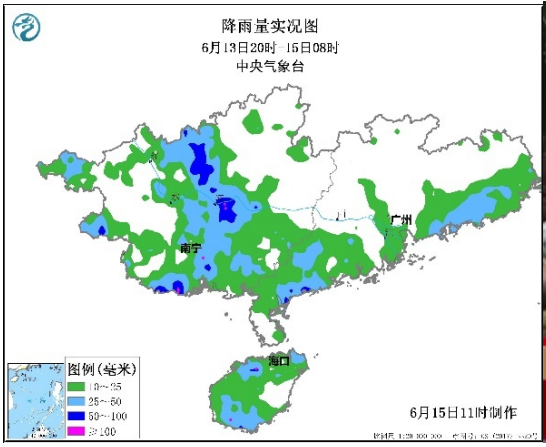

Fig 1.4c Actual Nuri Precipitation

Fig 1.4d Nuri Damages

(12UTC 13 June- 00UTC 15 June)

2) Typhoon Hagupit (2004)

Hagupit came into being over the waters to the east of Taiwan Island at 1200 UTC on 1 August before moving northwestward as a strong tropical storm at 2100 UTC on 2 August, then as a typhoon at 0600 UTC on 3 August. Hagupit made landfall over the coastal Leqing, Zhejiang around 1930 UTC on the same day (Scale 13, 38 m/s, 970hPa). It then moved farther northward to weaken into a tropical depression in Jiangsu at 2100 UTC on 4 June. Upon entering the western waters of the Yellow Sea, it intensified again into a tropical storm. On 5 August, it first weakened into a tropical depression at 1500 UTC and then converted into a subtropical cyclone before making landfall in the vicinity of Hwanghaenan-do of DPRK at 1900 UTC. It was ceased to be numbered at 2100 UTC on the same day.

Under the influence of Hagupit, the 3-5 August accumulated rainfall reached 100 to 280 mm in central and eastern Zhejiang as well as Shanghai; 300 to 350 mm in parts of Zhejiang like cities of Wenzhou, taizhou, Jinhua, Lishui and Jiaxing; 400 to 552 mm locally in Yongjia and Leqing of Zhejiang. Precipitation brought by Hagupit caused water to

rise above the warning levels of 20 rivers including the Ou, Jiao, Jinhua and Yong Rivers. Water rose above the highest safety levels at 24 hydrological stations and the Pinghu Station in the Hangzhou-Jiaxing-Huzhou area recorded the fourth highest water level. Besides, gusts in eastern Zhejiang, southern Shanghai, and southeastern Jiangsu reached Scales 8 to 10; in southeastern coastal Zhejiang, 11 to 13 and in one or two islands, 15 to 17. The highest wind speed of 59.8m/s (Scale 17) occurred at Hutou Isle, Dongtou, Zhejiang.

Hagupit affected Zhejiang considerably: several 100,000 people were relocated; 12,000 fishing vessels were called back to harbor; such industries as transportation, power supply, aquaculture, fishery and tourism were interrupted to varying degrees in eastern coastal Zhejiang. Severe waterlogging, villages submerged by abruptly rising water, and houses collapsed were found in many parts of Wenzhou.

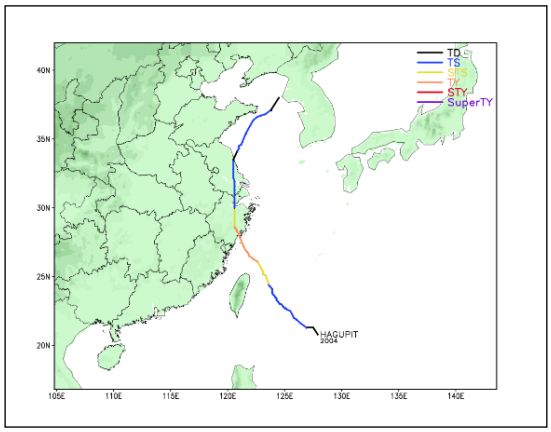

Fig 1.5a Track of Hagupit

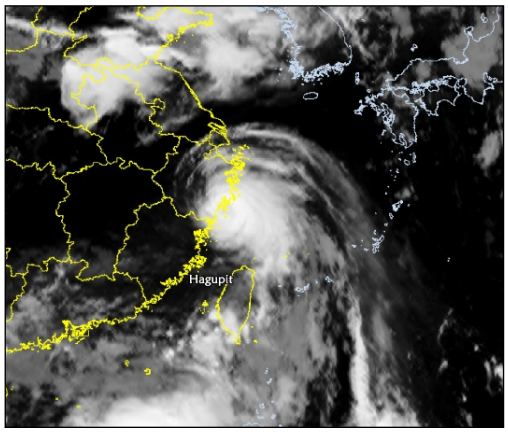

Fig 1.5b FY-4A Satellite Image of Hagupit

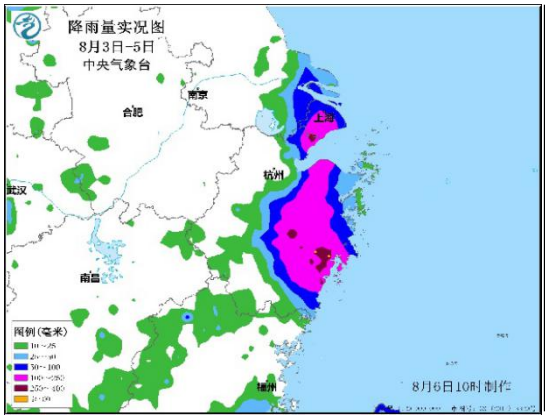

Fig 1.5c Actual Hagupit Precipitation

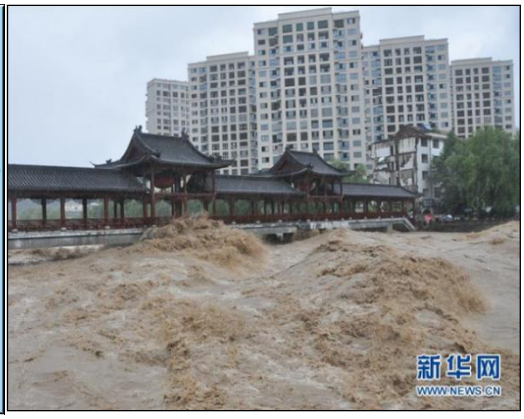

Fig 1.5d Hagupit Damages

3）Typhoon Higos (2007)

Typhoon Higos first formed over the northeastern waters of the South China Sea at 0000 UTC on 18 August. It moved then west by north while developing into a typhoon offshore central Guangdong at 1200 UTC on the same day. It made landfall over the coastal Jinwan District, Zhuhai City, Guangdong (Scale 12, 35m/s, 970hPa) around 2200 UTC. It continued its west by north movement after the landfall across southwestern Guangdong before entering eastern Guangxi as a tropical depression around 0930 UTC on 19 August. It was ceased to be numbered at 1500 UTC on the same day.

Under the influence of Higos, moderate and heavy rainstorms concentrated mainly in southern Guangdong, Pearl River Delta, and northeastern Guangxi. They were accompanied by gusts of Scales 7 to 10 and of 11 to 15 locally along the coast near the Pearl River mouth in Guangdong, with the highest (46.8m/s, Scale 15) registered on the Guangdong Xijiang Drilling Production Platform.

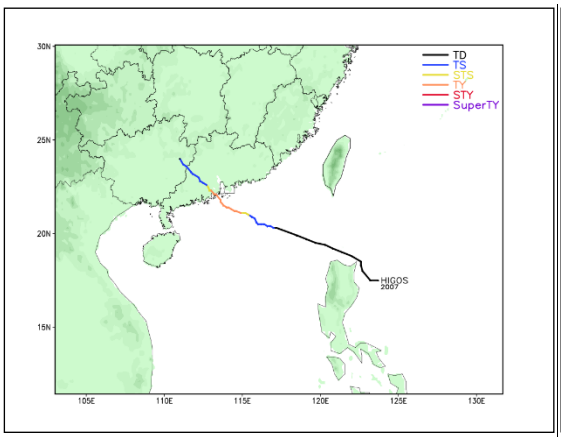

Fig 1.6a Track of Higos

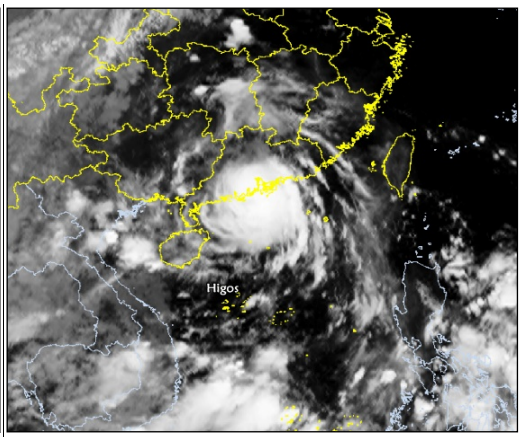

Fig 1.6b FY-4A Satellite Image of Higos

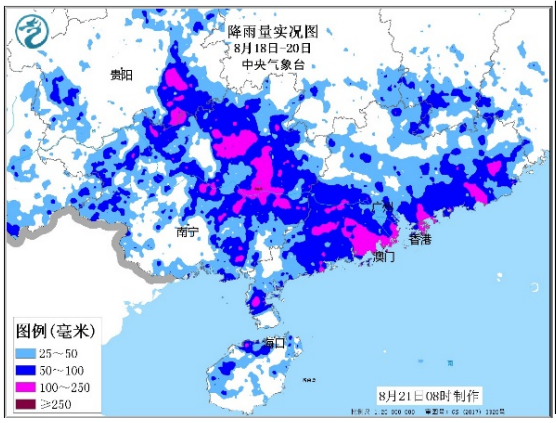

Fig 1.6c Actual Higos Precipitation

Fig 1.6d Higos Damages

(00UTC 18 - 00UTC 20 August)

4）Strong Typhoon Bavi (2008)

A tropical depression forming over the waters to the northeastern Philippines at 1200 UTC on 21 August grew into Tropical Cyclone Bavi (2008) over the eastern waters of Taiwan, China at 0000 UTC on the next day. While moving north by east, it intensified into a strong typhoon over the East China Sea at 0300 UTC on 25 August before moving by north into the northern Yellow Sea, getting weaker in intensity. Bavi made landfall over the coastal China and DPRK border province of North Pyongan (Scale 12, 35 m/s, 970hPa) around 0300 UTC on 27. It trod into Dandong of Liaoning as a weakening strong tropical cyclone around 0300 UTC, into Jilin at 0600 UTC, and reduced as a tropical depression in

Liaoyuan of Jilin at 0900 UTC. It was ceased to be numbered at 1200 UTC on the same day.

Under the influence of Bavi, downpours and rainstorms occurred in central-northern Jiangsu, western Shandong Peninsula, central-eastern Liaoning, most parts of Jilin, eastern and southern Heilongjiang; isolated heavy rainstorms in parts of Shandong and Liaodong Peninsulas, and in eastern Heilongjiang. A majority of the above areas registered accumulated rainfalls between 40 and 100 mm; parts of Shandong and Liaodong Peninsulas, between 120 and 200mm; Jimo of Qingdao, Shandong, locally between 250 and 342 mm; and Jidong County of Heilongjiang, 138 mm locally. Coasts in Jiangsu, Shandong Peninsula and Liaodong Peninsula measured strong winds of Scales 7 to 9 and gusts of 10 to 12.

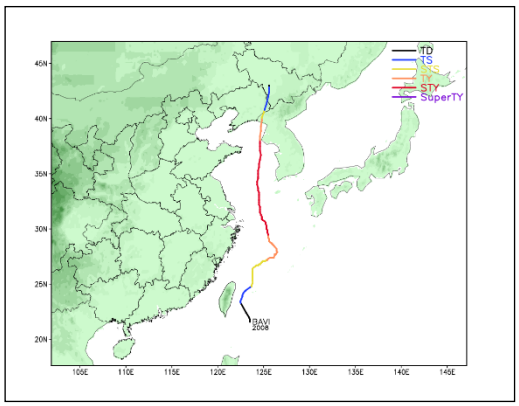

Fig 1.7a Track of Bavi

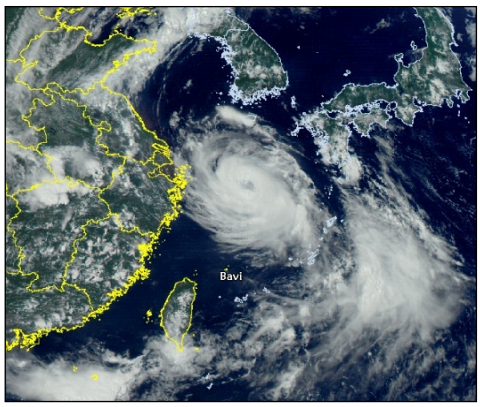

Fig 1.7b “Bavi”FY-4A Satellite Image of Bavi

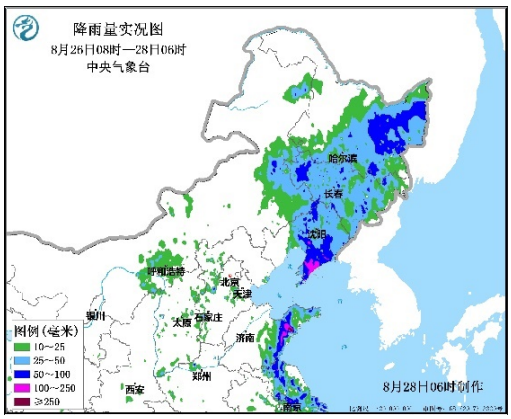

Fig 1.7c Actual Bavi Precipitation

Fig 1.7d Bavi Damages

(00UTC 26 - 22UTC 27 August)

5）Super Typhoon Maysak (2009)

Upon its genesis over the eastern waters of the Philippines at 0000 UTC on 28 August, the tropical depression moved southwestward. At 0900 UTC it intensified into Tropical Storm Maysak (2009). It started to move by north the next day and grew into a super typhoon at 2100 UTC on 31 August, the first of its kind in 2020. Maysak then started to move north by east, decreasing in intensity. It made landfall over the coastal Busan, South Gyeongsang Province, ROK around 1730 UTC on 2 September (Scale 14, 42m/s, 950hPa); and into Helong City, Yanbian Korean Autonomous Prefecture, Jilin China around 0540 UTC on the next day (Scale 8, 20m/s). It then turned in the northwest direction to reach Wuchang City, Heilongjiang (Scale 8, 18m/s) at 1200 UTC while converting gradually into a subtropical cyclone. Around 0300 UTC on 4 September it entered Hulunbuir, Inner Mongolia. It was ceased to be numbered at 0900 UTC on the same day.

Under the influence of Maysak, precipitation in parts of central-eastern Jilin and southern Heilongjiang exceeded 100mm: the 222mm at Panshi of Jilin and the 198 mm at Longjing of Yanbian marked the highest in Jilin; the 171 mm at Hailin of Mudanjiang and the 153 mm at Longjiang County of Qiqihar marked the highest in Heilongjiang. During the passing Maysak, daily rainfalls measured at 49 national observation stations in Jilin and Heilongjiang hit their highest records for September, among which two topped historical ones since their installation.

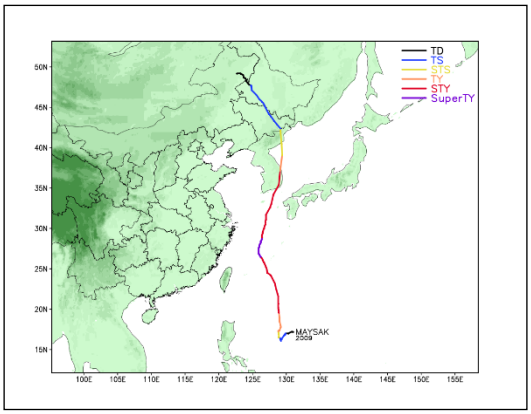

Fig.1.8a Track of "Maysak"

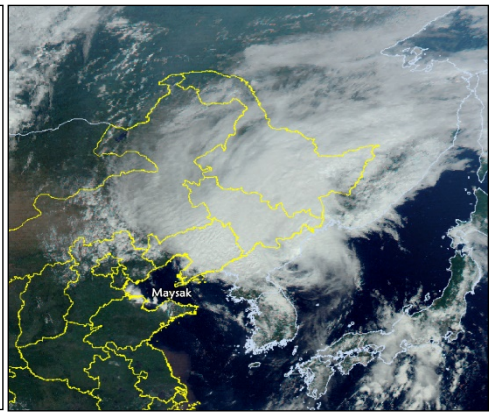

Fig.1.8b FY-4A Satellite Image of "Maysak"

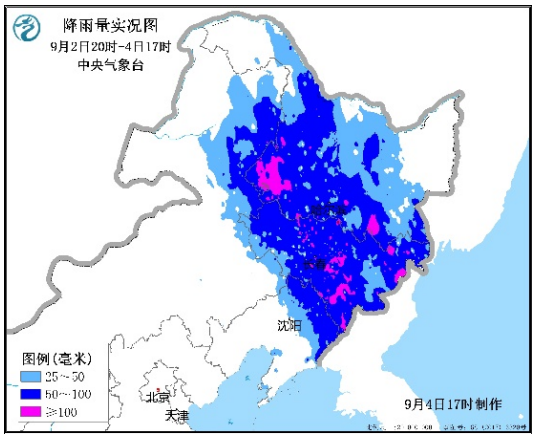

Fig.1.8c Actual "Maysak" Precipitation

Fig.1.8d "Maysak" Damages

(12UTC 2 September-09UTC 4 September)

6）Super Typhoon Haishen (2010)

Tropical Storm Haishen (2010) occurred first over the NW Pacific at 1200 UTC on 1 September, gradually intensifying as it moved in the northwest direction. It developed into a super typhoon at 2100 UTC on 3 September, turning from a northwest to a north by west movement. Then at 0300 UTC on 6 September it weakened into a strong typhoon. Haishen made landfall over the southern coast of ROK as a typhoon around 2330 UTC on the same day (Scale 13, 40m/s, 955hPa), across northeastern DPRK into Helong City, Jilin Province around 1800 UTC on the next day (Scale 8, 20m/s). It was ceased to be numbered in Dunhua of Jilin at 0000 UTC on 8 September.

The accumulated rainfall during its passage ranged from 50 to 150 mm in central-eastern Heilongjiang, Jilin, and eastern Liaoning, peaking 168 mm in Jilin at Quanhe Port of Hunchun and 152 mm in Heilongjiang at Suifenhe of Mudanjiang. Rainfall observed at 14 national meteorological stations hit their highest September records; daily rainfall at Suifenhe hit its highest historical record in Heilongjiang. Areas mentioned above witnessed accompanying gusts of Scales 8 to 9, with the highest wind speed of 27.8 m/s appearing at Dongning, Mudanjiang, Heilongjiang. Haishen and Maysak were highly overlapped in wind and rainfall impact zones.

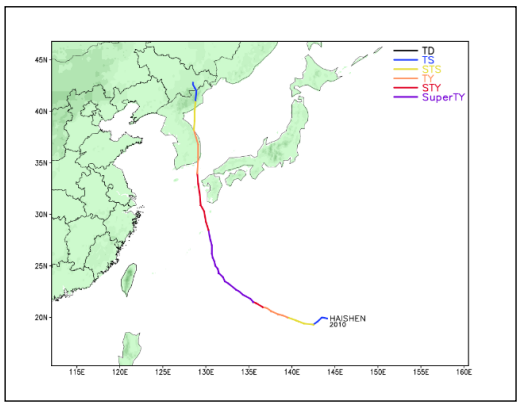

Fig.1.9a Track of "Haishen"

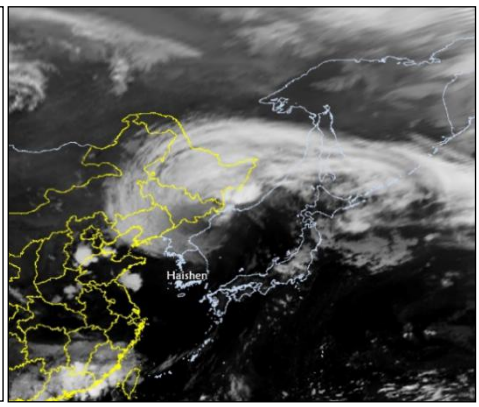

Fig.1.9b FY4A Satellite Image of "Haishen"

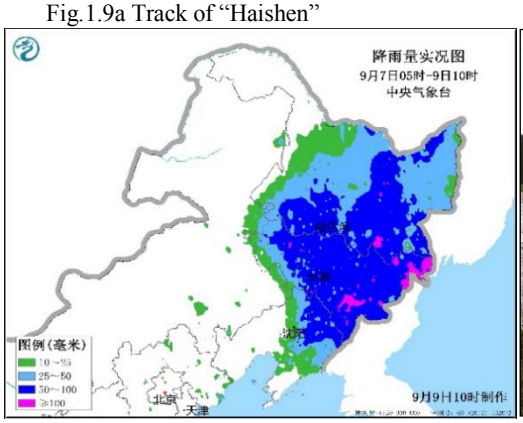

Fig.1.9c Actual "Haishen" Precipitation

Fig.1.9d "Haishen" Damages

(23UTC 6 Sept.-02UTC 9 Sept.)

7）Strong Tropical Cyclone Nangka (2016)

A tropical depression occurring over central-eastern South China

Sea at 0600 UTC on 11 October intensified into Tropical Storm Nangka (2016) over central by east South China Sea at 0000 UTC on 12 October. Continuing its west by north movement, Nangka became a strong tropical storm over NW South China Sea at 0300 UTC and made landfall over coastal Qionghai, Hainan with decreasing intensity around 1200UTC on 13 September (Scale 10, 25m/s, 988hPa). Around 1630 UTC it moved from Hainan Island to Beibu Gulf as a tropical storm; and around 1020 UTC the next day it made its second landfall over the coastal Thanh Hoa, Vietnam (Scale 8, 18m/s, 998hPa) with weakening intensity. It was ceased to be numbered at 1500 UTC on the same day.

Under the influence of Nangka, from 0800 UTC 12 to 0800 UTC 15 October, eastern and northern Hainan, southwestern Guangdong and southeastern Guangxi were hit by gusts of Scales 6 to 8; offshore islands, eastern and northern Hainan, and Zhanjiang of Guangdong Province, isolated gusts of Scales 9 to 11. The highest wind speed (Scale 11), 30.4 m/s, appeared at Qizhou Archipelago of Hainan. Accumulated rainfalls ranged from 100 to 200 mm in parts of eastern Hainan, southwestern Guangdong, and central and southern Guangxi; from 250 to 320 locally in Haikou and Qionghai of Hainan, Zhanjiang and Maoming of Guangdong, and Fangchenggang of Guangxi; peaked 346 mm locally in coastal Maoming, Guangdong. Under the impact of strong precipitation accompanying Nangka, 5 small and medium-sized rivers in Guangxi, including the Zuojiang tributaries of Mingjiang, Gong'an and Sizhou Rivers, the Youjiang tributary of Lushui River, and the southern coastal river of Beilun, had water rises above their warning levels by 0.36~1.15m.

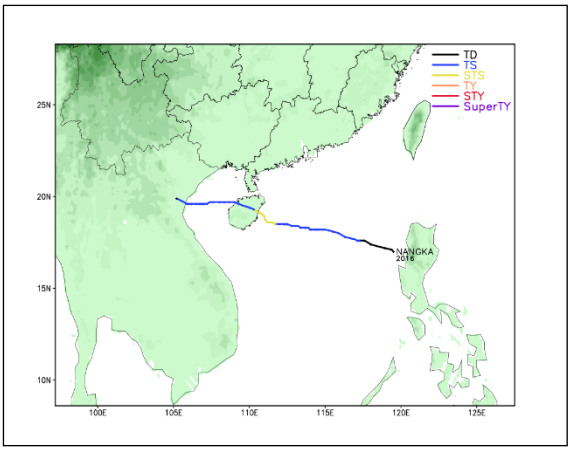

Fig.1.10a Track of "Nangka"

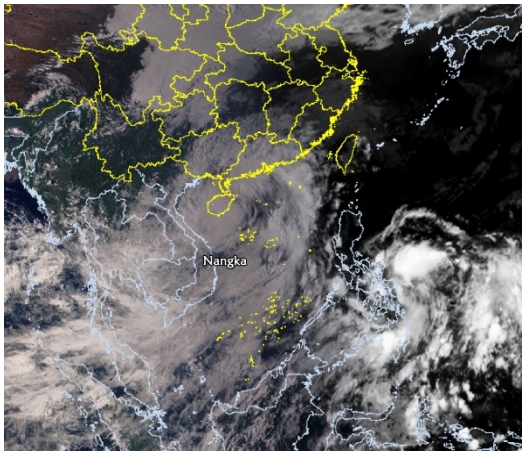

Fig.1.10b FY4A Satellite Image of "Nangka"

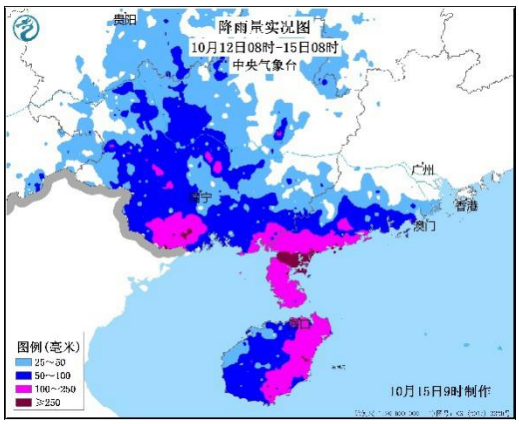

Fig.1. 10c Actual "Nangka" Precipitation

Fig.1.10d "Nangka" Damages

(00UTC 12 Oct.-00UTC 15 Oct.)

1.1.5 TC Climate Prediction

The National Climate Centre (NCC) undertakes a seasonal prediction on the number of tropical cyclones forming over the South China Sea and the NW Pacific, their landing frequency in China, possible path and intensity in March and May each year, mainly based on a combination of physical statistics and dynamic models.

1) Year-Round TC Prediction

It is estimated that 26 to 28 TCs will be born over the NW Pacific and the South China Sea waters in 2020, slightly more than the normal-year number of 26. It is estimated that 7 to 9 TCs will land in China, slightly more than the normal-year number of 7. The landing TCs are estimated to be strong, follow mostly northwest paths, and be likely to

move northward. TC activities indicate that more TCs are born at a later than an earlier stage and they are more active from late summer to early autumn than in normal years.

2）Summer Tropical Cyclone Prediction

It is predicted in May 2020: 8 to10 TCs will occur over NW Pacific and South China Sea this summer, fewer than the normal-year number of 11; 4 to 5 of them will land in China, leveling off with the normal-year number of 5.

The actual case is that 8 TCs occurred last summer and 4 of them landed in China, approximately the same as predicted.

1.2 Socio-Economic Assessment

China was affected by 9 TCs this year, 5 of which made landfalls over the mainland. They afflicted a total of 10.599 million people in 11 provinces, caused 8 deaths and 559,000 relocations, brought down 8100 and damaged 59,000 houses, injured 3,858,600 and destroyed 169700 hectares of crops.

From late August to early September, three TCs moved farther north one after another to affect NE China, namely, the No. 8, 9 and 10 Bavi, Maysak and Haishen. They appeared at short intervals and were highly overlapped in impact zones. Under the influence of these TCs and their peripheral cloud patterns, the half-month average rainfall in NE China reached 170.1 mm, three times more than the normal-year record; major rivers, including Neng, Songhua and Heilong Rivers, had water rises above warning levels. Statistics had it that the three TCs affected a total of 8.396 million people in Inner Mongolia, Liaoning, Jilin, Heilongjiang and Shandong; caused 124,000 relocations; and brought down 3600 and damaged 49,000 houses. Besides, No. 4 TC Hagupit landing in Zhejiang, which was marked by quick movement, rapid development, great power, and severe destruction, caused 5 deaths.

Table 1 TCs Landing in China and Damages Caused in 2020

Name and Code	Landing Location	Landing Time and Intensity	Provinces Hit	Population Afflicted (10,000)	Deaths /disappearances	Population Relocated (10,000)
Nuri (2002)	Yangjiang, Guangdong	14 June (tropical storm)	Guangdong, Guangxi	2.9		0.1
Sinlaku (2003)			Guangdong, Guangxi	3.1		0.03
Hagupit (2004)	Wenzhou, Zhejiang	4 August (Typhoon)	Shanghai, Zhejiang	187.8	5	32.7
Mekkhala (2006)	Zhangzhou, Fujian	11 August (Typhoon)	Fujian	5.9		4.4
Higos (2007)	Zhuhai, Guangdong	19 August (Typhoon)	Guangdong, Guangxi	15.2	3	4.8
Bavi (2008)			Liaoning, Jilin, Heilongjiang, Shandong	48.0		3.6
Maysak (2009)			Inner Mongolia, Liaoning, Jilin, Heilongjiang	686.3		3.6
Haishen (2010)			Liaoning, Jilin,	105.3		5.2

Name and Code	Landing Location	Landing Time and Intensity	Provinces Hit	Population Afflicted (10,000)	Deaths /disappearances	Population Relocated (10,000)
			Heilongjiang			
Nangka (2016)	Qionghai, Hainan	13 October (Strong Tropical Storm)	Guangdong, Guangxi, Hainan	5.5		1.4
TOTAL				1060.0	8	55.83

1.3 Regional Cooperation Assessment

1.3.1 Data Support to Bangladesh

The strong cyclonic storm Amphan born at the Bay of Bengal developed into a super cyclonic storm on the evening of 17 August. At 0800 UTC the next day the storm was centrally located about 1060 km south by west to Calcutta of India over southern Bay of Bengal, i.e., 13.1°N, 86.4°E, with a highest near-center wind force of Scale 16. Bangladesh Meteorological Department (BMD) contacted the World Meteorological Centre Beijing (WMC-Beijing) via CMACast, expressing a wish to have real-time access to China's high-resolution NWP products for guidance. On the morning of 18, WMC-Beijing brought together experts from the National Meteorological Centre (NMC) to open a dedicated account for BMD on its high-speed meteorological data exchange website, enabling real-time access to FY4A satellite images, GRAPES-GFS and the NMC globally refined gridded forecast products.

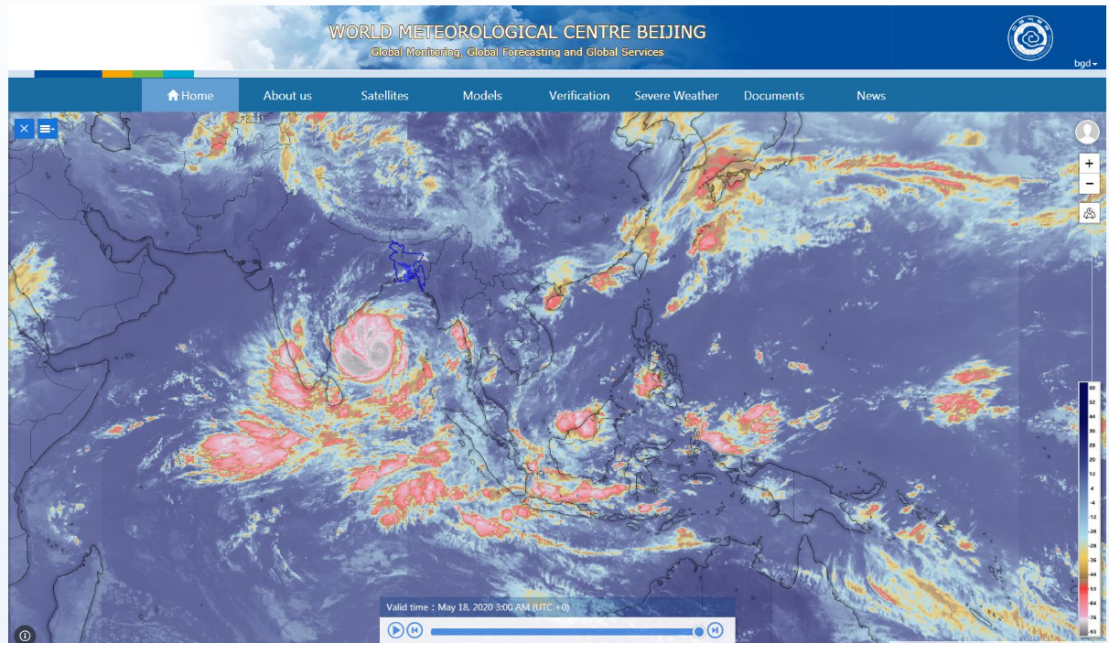

Fig.1.11 WMC-BJ Real-Time Data

1.3.2 Advances in *Tropical Cyclone Research and Review* in 2020

By October, three issues of *Tropical Cyclone Research and Review (TCRR)* have been published this year. At present, TCRR is working through KeAi Publishing Communications Ltd. with the worldly-known publisher Elsevier BV to boost its citations. Elsevier's private list is leveraged to make irregular promotions of the top download articles, the e-journal and Editor's Selection. TCRR-related news is released via social media as well.

TCRR has been indexed in the Emerging Source Citation Index (ESCI, a database produced by Clarivate as is SCI) , and in the three full-text databases of the Elsevier ScienceDirect, the DOAJ launched by Lund University of Sweden in 2003, and CNKI - the most comprehensive academic source in China. Therefore, free full-text downloads are not only available at the official TCRR website but also the three full-text databases mentioned above. Currently, TCRR has a wide audience in 126 countries and regions around the world. TCRR has registered 50000 full-text downloads for three consecutive years, and over 53000 downloads for the first eight months of 2020.

II. Progress in Key Research Areas

2.1 Application of Machine Learning (ML) in TC Intensity Estimation

In cooperation with Alibaba DAMO (Discovery, Adventure, Momentum and Outlook) Academy, NMC has been experimenting on the ML-based TC intensity analysis, with good effects seen.

Amid the AI fervor, ML technology, which is being widely applied in all walks of life, turns out to be very effective in solving many technical problems. This is manifested in TC forecasting by applying satellite images in offshore TC intensity estimation. Starting from the 1980s, TC intensity estimation has been made in the top facilities based on DVORAK analysis and the subsequently developed ADT and AODT, the idea of which is the same as DVORAK. The Dvorak tropical cyclone intensity estimation technique is likely to lead to big errors when it comes to TCs with rapidly fluctuating intensity, of over-large or over-small scale, and of fast motion. However, satellite image-based TC intensity estimation is recognized as a classic classification for AI given its maturity in underlying technology, which accounts for our initiative in this connection to offer an objective reference for TC operation.

Deep learning is used to construct the Network Architecture Search based representation learning network (or convolutional neural network, CNN) for identification of TCs from satellite images and for efficient and accurate estimation of the TC center wind speed and pressure using information on the TC center's longitude and latitude and the best track position and intensity in combination with the logistic regression and image search techniques (Fig. 2.1a). Given its high computability,

scalability and security, this system can be very promising in fast interpreting meteorological satellite data, extracting effective information from the images and cutting down labor cost. The validation set of isolated TC samples indicates that this TC intensity estimation model strikes a mean absolute velocity error of 4.1 m/s (Fig.2.1b). Work to be done includes further verification of and improvement on the model based on individual 2020 TCs.

Contact Information: National Meteorological Centre

2.2 Advances in Typhoon Numerical Modeling

1) GRAPES_TYM Upgrade Accomplished. GRAPES_TYM upgraded by NMC in August 2019 includes: horizontal and vertical resolutions raised from 0.12°/L50 to 0.09°/L68; forecast coverage expanded from NW Pacific and South China Sea to also the north Indian Ocean (0°E-180.04°E, 15°S-60.06°N, Fig.2.2); lead time extended to 120h, forecast 4 times/day. GRAPES_TYM forecasts of the 16 tropical cyclones by 18 October 2020 strike a mean 72h path error of less than 186km and a near-surface maximum wind speed error ranging between 3.5-6 m/s (Fig.2.3).

2) GRAPES-GFS Upgraded to V3.0. Major improvements include: 1) a new dynamic core generated for GRAPES-GFS by incorporating the three-dimensional reference atmosphere and the estimation-adjustment semi-implicit semi-Lagrangian (SISL) time integration scheme to optimize and adjust the dissipative terms in the model for improved computation accuracy and stability, and for enhanced calculation efficiency by enlarging the time step (dt); 2) vertical stratification increased from 60 to 87 layers with the top one raised from 10hPa to 0.1hPa based on the new dynamic core; 3) stratosphere simulation significantly improved with the addition of the non-orographic gravity wave process and near-top relaxation algorithm; 4) cloud physics simulation of tropopause enhanced using the optimized ice-surface saturated specific humidity calculation formula; and 5) orographic filtering improved and high-precision terrain modeling adopted. A new vortex initialization scheme was developed based on the data assimilation technology. With a forecast experiment carried out using the 2019 tropical cyclones 1904-1920, it was found that the new scheme can help boost GRAPES-GFS TC path forecasting and significantly improve

intensity estimation (center pressure and near-surface maximum wind speed). Incorporated into the operational system at the end of July 2020, the new scheme has succeeded in predicting 16 tropical cyclones this year.

3) TRAMS Model Enhanced. In 2020, TRAMS uplifted the 3D reference atmosphere based high-resolution dynamic core by incorporating a new horizontal diffusion scheme, enhancing the Lagrangian Advection Algorithm, redeveloping the iterative SISL scheme, while optimized the access to the functional blocks of model's dynamic physical process plus some technical parameters, and developed the cloud precipitation physical, sea and land surface and PBL parameterization schemes well suited to the low latitudes. TRAMS technical improvement mainly tackles the small-scale disturbances triggered by the high resolution for higher forecasting accuracy and stability, while parameterization scheme uplifting aims to effectively raise precipitation forecast accuracy at various magnitudes and significantly reduce surface element forecast error.

Also, TRAMS adopted one-way Barnes analysis in its updated new positioning algorithm. The old version calculates the typhoon center position based on one variable while the new one performs Barnes analysis of the variables before deriving such a position from weighted averaging of the extreme positions of three variables. Batch testing of the 2020 TCs indicates that the updated positioning program turns out to be more accurate than the old one at different timelines (Fig. 2.4).

4) TEDAPS made accessible to National Operation. The mesoscale WRF and GSI 3DVAR-EnKF based Typhoon Ensemble Data Assimilation and Prediction System (TEDAPS), which features ensemble data assimilation, makes ensemble typhoon forecasts by assimilating data of various sources, such as conventional, TC Vital and satellite, in a

hybrid manner, before using a combination of the initial disturbance and multi-parameterization schemes. TEDAPS was put under a quasi-operational test in 2015 and into official operation in Shanghai Meteorological Service (SMS) in 2019. Having been permitted this year to enter into full operation, TEDAPS stands out as the first ensemble typhoon forecast system to be part of the national weather broadcasting. It is activated at 0800 and 2000 each day for 72h forecasts with 21 members to offer a good variety of deterministic and ensemble probabilistic forecast products of typhoon path, intensity and hit chance as well as accompanying wind and precipitation. The general performance of TEDAPS was evaluated in the years of 2016-2019 to reveal that it is comparable to NCEP GEFS in terms of track prediction error and that it beats GEFS in terms of intensity prediction (Fig.2.5).

5) TRANSv1.0 Put under Quasi-Operation. Typhoon Rapid Refresh Analysis and Nowcasting System (TRANS v1.0) was co-developed by the NMC, Guangzhou Institute of Tropical and Marine Meteorology (ITMM) and Nanjing University under the aegis of CAMS. It integrates key technologies such as the EnKF sequential radar data assimilation, SETM, and targeted typhoon assimilation sensitive area identification. In this regard, it is an effective boost to the applicability of high temporal and spatial resolution pre-landfall radar observations to typhoon numerical modeling. The verification and evaluation of the 3-year (2017-2019) batch test on TRANS v1.0 indicate that it performs well in predicting the path and intensity of a TC being about to make landfall, making fine depiction of small and medium-scale precipitation processes, forecasting how precipitation intensity evolves while generating gust and wind forecast products with high temporal and spatial resolution. Approved on 6 August 2020 by the CMA Department of Forecasting and Networking for quasi-operation, TRANS v1.0 has

generated as of 20 October 2020 real-time forecasts of 6 landing typhoons. Its operation in a real-world environment proves to be stable and reliable; its lead time meets current operational needs; its forecasting products have been used in many national forecast discussions in particular typhoon focused ones (Fig. 2.6).

6) Typhoon-Specific Air-Sea Coupling Model and Parameterization Scheme Developed. The air-sea interaction between the typhoon and the ocean has a great influence on typhoon intensity structure. A regional air-sea coupling model for operational forecasting of TCs in NW Pacific has been built by CAMS to study the impact of the interaction between typhoons and the ocean, with a typhoon-specific physical parameterization scheme developed. In this scheme, the three physical processes of vertical mixing, advection and heat retrieval in the ocean are parameterized, with sea surface height and ocean subsurface information added. This scheme, which simulates the changing ocean surface only but quickly, is well suited to operational forecasting of typhoons.

Contact Information: National Meteorological Centre
Guangzhou Institute of Tropical and Marine Meteorology
Shanghai Typhoon Institute
Chinese Academy of Meteorological Sciences

2.3 FY Satellite-Based Typhoon Monitoring and Disaster Pre-Evaluation

Based on Fengyun meteorological satellite and other auxiliary data, a satellite-based typhoon hazard factor extraction algorithm has been established as part of a disaster monitoring model to designate dynamic critical indicators of the hazard factors for different seasons and different locations, including 10 typhoon ones under 4 categories and 6 quantitative indicators of victims and damages under 4 categories. On the one hand, this is an innovation in that the traditionally intensity- and path-focused typhoon monitoring and forecasting are moving further to quantitative wind and rain parameters related to typhoon intensity, location and scale. At the same time, the relationship is established between these parameters and the ones that actually characterize a given disaster. On the other hand, a one-dimensional variational inversion algorithm has been established based on the microwave data from the Fengyun polar-orbiting satellites as a monitoring method for such hazard factors as typhoon intensity, precipitation, temperature and humidity profiles to effectively address precipitation pollution on the microwave instruments in the middle and low layers, enabling more accurate structure detection. An integrated quantification algorithm with a display platform has been established for typhoon structure, intensity, and wind and rain impacts to be applied in discussions and analyses during emergency responses for typhoons in 2020, including Hagupit, Higos, Bavi, Maysak and Haishen. The Fengyun meteorological satellite-based typhoon and hazard assessments contribute to the accurate monitoring of typhoons as well as the pre-evaluation of typhoon damages, a step forward by FY satellites as a forecast enabler in addition to a monitor.

Contact Information: National Satellite Meteorological Center

2.4 Typhoon Field Observation Experiments

1) Successful Implementation of Haiyan Project

Haiyan Project was launched by CMA to promote marine typhoon observation and forecast services. Its primary task is to focus on typhoon monitoring and warning services in the South China Sea, taking into account the ecological needs of meteorological services in the Qinghai-Tibet Plateau and the upper reaches of the Yellow River. Thanks to China's independently-developed large-scale UAVs, this project is intended to establish an operational space-based mobile observation plus a technological innovation and cooperation platform to meet the needs of the meteorological observation, numerical forecasting, scientific research, social services and international cooperation to give full play to its social and economic benefits.

From June to August 2020, CMA Meteorological Observation Center (MOC) conducted in the South China Sea a high-altitude large-scale UAV-based comprehensive marine meteorological observation experiment in cooperation with 12 stakeholders. Yilong-10 large-scale UAVs were employed to carry independently-developed drop sondes and millimeter wave radars. One solar-powered unmanned boat and two drifting buoys were deployed in the designated sea area and intelligent round-trip sondes at the Sansha Weather Station as an integrated three-dimensional observation network for the South China Sea. From 31 July to 2 August, the system carried out its virgin mission to observe the formation and evolution of Typhoon Sinlaku in a three-dimensional fashion and successfully capture the South China Sea low pressure and the changing meteorological and marine elements observed before and after the passing Sinlaku. Observations of 21 elements, which were obtained with 5 types of sea, air and space

equipment, ranged from the profiles of temperature, humidity, wind, pressure, cloud and atmosphere of 10km upper-air down to sea surface to air temperature, humidity, wind, sea temperature and sea salt at sea-surface level, which were transmitted real-time to MOC's aircraft data processing and commanding system while those from the drifting buoys and on the equipment operating conditions to MOC to be processed and displayed via the updated integrated product system for meteorological observation (Tianyan) and the developed operational marine meteorological observation system. The measured data were then analyzed in comparison with satellite observations from both home and abroad and those from various models using robust data quality control techniques to derive how meteorological and marine observation elements respond to a typical typhoon weather process. The experiment-derived data, which provide important support to typhoon location and intensity determination, help to improve the prediction accuracy in this connection. The campaign is rated as a milestone in the analysis of typhoon structure and its impacts on the South China Sea, the promotion of the numerical model application, and the evolution of UAV weather observation, an initiative that has filled up the gap of upper-air large scale UAV-based integrated marine meteorological (typhoon) observation in China. Such data have been reviewed and found to be qualified for operational use. Those applied in numerical models indicate that they can improve the background field of the models and raise the Ts score of the 24-hour precipitation forecast by about 3% (Fig. 2.7).

2) Typhoon Higos Observation Experiment

According to the "*Integrated Typhoon and Gale Hazard Monitoring and Warning - Key Technology R&D and Demonstration*" – a research study listed in the Guangdong provincial key-area R&D project program, Typhoon Higos field observation experiment was conducted in

Guangdong in the cities of Shenzhen and Zhuhai and at CMA Marine Meteorological Science Experiment Base (MMSEB) at Bohe in August 2020 to obtain the boundary layer and turbulence characteristics of landing typhoons. This experiment generated data observed by wind profile radar, by-second AWS, buoy, tidal gauge, and weather gradient tower.

3) Collaborative Typhoon Nangka Observation Experiment

Based on a national key research and development project entitled "Offshore Typhoon 3-D Collaborative Observation Scientific Experiment" and EXOTICCA, CMA STI, in cooperation with Hainan Provincial Meteorological Service and Hong Kong Observatory (HKO), conducted from 12 to 14 October 2020 the first multi-platform collaborative typhoon observation scientific experiment on Typhoon Nangka (2016) over the central/northern South China Sea (near Qionghai) successfully (Fig. 2.8 shows medium and high-altitude UAV flight route and observation height vector wind).

In this experiment, the collaborative multi-platform observation was conducted throughout the typhoon process, integrating the land-based (wind chasing vehicles and ground automatic stations, conventional stations, etc.), sea-based (unmanned boats, offshore buoys, etc.), sky-based (high, medium, and low-altitude drones carrying lidar and dropsondes for observation), and space-based (FY-4 satellite continuously intensive observation) facilities. Data obtained include: by-second observations of wind, temperature, humidity and pressure in the periphery and core areas before and after the typhoon landfall. Another pilot experiment was conducted successfully, i.e., "secondary sounding" (A small parachute, which is ejected from the falling payload from the burst sounding balloon, completes a second sounding), with a large amount of valuable data gathered. The rare scientific data set

obtained in this experiment is of important scientific significance to a better study of typhoon mechanism and the numerical model improvement.

Contact Information: National Meteorological Observation Center
Guangzhou Institute of Tropical and Marine Meteorology
Shanghai Typhoon Institute

2.5 Advances in TC Scientific Research

1) Impact of Environmental Fields on MPI of TCs. TCs are theoretically proved to have maximum potential intensity (MPI), which is defined as the maximum intensity that TC can reach under given favorable marine and atmospheric thermal conditions. Widely used in operational forecasting and climate analysis, MPI, which is often believed to be determined by SST, may vary under the same SST due to the different atmospheric environment backgrounds. The best track and reanalysis data were applied to a MPI analysis of the 1980-2015 North Atlantic TCs to figure out the contribution of TC atmospheric circulation field to MPI variance. It was found that under a given SST the change between the 10th and 90th percentile medians of MPI samples can reach 10-15m/s, accounting for 20-25% of the median MPI under the same SST. It was also found that higher (lower) MPIs occur in drier (wetter) and colder (warmer) atmospheric environments. lower SST MPI is more sensitive to atmospheric temperature whereas higher SST is more sensitive to boundary layer humidity. Moreover, a comparative study of the MPI differences between the Atlantic, Eastern Pacific, NW Pacific and North Indian Oceans reveals that under the same SST condition NW Pacific MPI is lower than the East Pacific MPI. This can be attributed mainly to the relatively warmer troposphere and wetter boundary layer over the west Pacific (Fig. 2.9).

2) Contributors to and Sensitivities of the TC Weakening at Sea. Reanalysis data and machine learning methods were used to analyze the rate of NW Pacific TCs weakening at sea during the 1980-2017 typhoon seasons, rapid weakening contributors in particular. It was found that TC rapid weakening events usually occur when intense TCs cross regions with a sharp decrease in sea surface temperature (DSST) and move with

relatively faster speeds into regions with a large environmental vertical wind shear (VWS) of dry conditions in the upshear-left quadrant. Sensitivity diagnosis and analysis indicate that the relative intensity of TC (TC intensity normalized by its maximum potential intensity), DSST, and VWS are dominant factors, contributing 26.0%, 18.3% and 14.9% respectively to the TC weakening rate. The contribution of other factors was limited. These findings suggest that the improved accurate analysis and prediction of the dominant factors may lead to substantial improvements in the prediction of TC WR. (Fig. 2.10).

3) Against the backdrop of climate change, landing TCs tend to have stronger intensity, longer duration after landing and more rainfall upon landing over the southeastern coast. A statistical analysis of the best track data and global reanalysis data of the 1980-2018 TCs indicates that landing TCs display a trend of growing PDI (Power Dissipation Index) over the past few decades (Fig. 2.11). This can be attributed mainly to an average northward shift of the TC landing points, a longer sustaining time on land caused by lower TC weakening rate. A further analysis suggests that this change is related to the increase in offshore sea temperature, the increase in temperature and humidity of the underlying land surface, and the decrease in low-level wind shear. Landing TCs brought significantly more precipitation to the coastal southeast and slightly less to the south over the same period of time. This can be attributed mainly to the northward shift of the overall weak TCs in frequency and density and to increased precipitation in frequency and intensity in the southeast caused by longer TC sustaining time on land. Despite an overall precipitation decrease, South China witnessed an increase in precipitation sent by strong typhoons, caused mainly by the abundant water vapor and prolonged TC durations on land.

4) Raindrop size-based study of the microphysical process of

typhoon cloud. Based on data gathered with 9 ground disdrometers in northeastern Fujian, a comparative study was made of the raindrop size distribution (RSD) characteristics of the convective inner-rainband rain (CIR) and convective outer-rainband rain (COR) accompanying Typhoon Maria (2018). It was found that the radar reflectivity for the CIR increases sharply with decreasing height below the melting layer whereas it remains nearly unchanged for the COR. This suggests that the collision-coalescence process plays a significant role in the case of CIR. The reason is that the closer to the TC center (with the decrease in radius), the greater the vortex ascending motion is, preventing small raindrops from falling to the ground while some held aloft are collected by large falling raindrops. Thus, the surface-level CIR generally has far lower concentration of small raindrops and larger mean raindrop diameter (Dm) than those found in the COR. Besides, it was found for the first time that although the raindrops close to the TC eyewall are relatively large on average, the raindrop concentration is too low to yield a high rain rate. In contrast, high rain rates are concentrated at a distance of about 1.5-2.5 times the radius of maximum wind from the TC center, where there are appropriate concentrations (log10Nw) and corresponding raindrop diameters (Dm). Last but not least, this study confirms the existence of different microphysics between the CIR and COR in terms of the radar reflectivity-rain rate (Z-R) and shape-slope (μ-Λ) relationships (Fig. 2.12).

5) Predictability of Numerical Models to Typhoon Lichma Landing Precipitation Assessed. A comparative study was made to show how effective the numerical model is in the prediction of Typhoon Lichma (2019) precipitation at different landing stages (upon landfall, deep inland northward). It was found that the model performs better in predicting convective precipitation upon landfall than at the stage of

inland penetration, a result related mainly to model's ability to predict the interaction between the typhoon and the westerly trough system. The model failed to predict the asymmetric structure of precipitation at the time of typhoon landfall; and as the typhoon penetrated deeper inland northward to interact with the mid-latitude westerly belt system, it failed again to predict the heavier precipitation due to its weakness in forecasting the frontal intensity (Fig. 2.13).

6) Impact of Dropsonde Data Assimilation on Mangkhut Forecasting. The impact of dropsonde assimilation on typhoon forecast based on data from 9 dropsondes released in the storm's northwest quadrant by HKO at 1000 UTC and another 5 at 1200 UTC on 15 September 2018. The resulting data of the experiment showed the typhoon's circulation weakening at lower levels and strengthening at middle levels, and an intensification of the asymmetry of the typhoon's horizontal kinematic structure between its eastern and western parts after the assimilation of dropsonde data. In addition, water vapour over the northwestern side increased from lower to middle levels, and the warm-core structure was further strengthened. The dropsonde data assimilation resulted in improved quantitative precipitation forecasts during landfall: the averaged track error in the DROP was > 10% lower than in the non-assimilation case; and the maximum surface wind speeds and minimum sea level pressures were all closer to those observed before landfall (Fig. 2.14).

Contact Information: Chinese Academy of Meteorological Sciences
Guangzhou Institute of Tropical and Marine Meteorology
Shanghai Typhoon Institute

2.6 Enhancement of Typhoon Disaster Emergency Rescue

1) Strategic Arrangements in Advance, Elaborate Service, Cooperation and Coordination. CMA issued a special notice (*"Notice on Preparing for Meteorological Services in the Flood Season in 2020"*) to require Provincial Meteorological Services and affiliated agencies to start 1 March careful preparation for the meteorological service operations in the 2020 flood season, during which CMA issued a joint notice with the Ministry of Natural Resources, making strategic arrangements on the forecasting and warning of geological disasters and meteorological hazards. Regular consultation meetings were held with the State Flood Control and Drought Relief Headquarters (SFCDRH), the Ministry of Emergency Management (MEM), the Ministry of Water Resources (MWR) and the Ministry of Natural Resources (MNR) to ensure in-depth integration of meteorology into flood control and disaster relief command and dispatch operations. At local levels, meteorological services worked closely with their water and natural resource counterparts in issuing meteorological warnings for flash floods and geological disasters. Communication, coordination and collaboration with the transport, culture and tourism, and city operators and managers were activated to jointly study and judge typhoon impacts on tourism, arterial transport and power supply infrastructure, and production safety.

2) Boost to Emergency Management Capacity. MEM conducted in late May a national disaster information officer training online via video, in which a total of more than 70,000 trainees specialized in damage management participated. Being well designed to incorporate policy interpretation, case studies, and hands-on practices, the event ensured a truly rewarding experience for the trainees. The project turns out to be an effective boost to risk and damage management skills of

local officers at various levels.

3) Improved Disaster Information Management. The national disaster reporting system has been in operation for 12 years, providing disaster information officers at all levels across the country with a unified collection and reporting tool in this connection that integrates desktop and client terminals and with a reliable and stable IT support environment. The system also supports seamless access to the unified domain name portal and APP, and provides data, reports, and on-site photo submission services. Based on the disaster reporting system, a 6-level damage information delivery system of "country-province-city-county-township-Village" was formed to standardize the routine processes of bottom-up collection and submission of damage information and its top-down summary review. The disaster reporting has been continuously improved in timeliness and quality, a practice that has played an important supporting role in the responses to catastrophic disasters such as typhoons. Up to now, MEM has received more than 99,000 bulletins of damage information from its line departments at all levels.

Contact Information: National Disaster Reduction Centre, Ministry of Emergency Management of the People's Republic of China

Department of Emergency Response, Disaster Mitigation and Public Services, CMA

2.7 Renaming Yutu - a Public Science Awareness Promotion Event

Last September the Central Meteorological Observatory (CMO) held a typhoon name-giving event on the new media platform, aiming to solicit a new name to replace the delisted Yutu for Typhoon No. 26 in 2018. This is the second time that the typhoon naming right has been given to the public and individuals, the first being three years away. The campaign was started with a media briefing followed by a Q&A session as an official announcement of the event while details on typhoon naming and de-listing rules provided in addition to an overview of 2020 typhoons and their activities. Meanwhile, a multi-platform joint online live streaming of the lot-drawing ceremony for the typhoon naming right, scientific outreaches about typhoon went on Weibo, WeChat and other new media. This event became immediately the focus of major mainstream media outlets and the public. Popular science articles on the same topic had an audience of 180 million with 162,000 comments. More than 10,000 Chinese netizens participated in the typhoon naming process. In the end, three were selected by experts from the names submitted by netizens to be made known to the public. They will be presented by China to the Typhoon Committee in due course of time (Fig. 2.15).

Contact Information: National Meteorological Centre

2.8 CMA-sponsored Training on Skills in TC

Over the past year, CMATC has conducted a number of physical and distant trainings on TC operational skills in a bid to enhance forecasters' ability and promote the application of new techniques and new data in typhoon forecasts.

1）The 69th Weather Forecaster Competency and Capacity Training A (Short-Range Forecasting) - Online

The 69th Weather Forecaster Competency and Capacity Training A (Short-Range Forecasting) - Online was held by CMATC from July to December 2020, an online event that was conducted on the China Meteorological Distance Education Network (CMDEN). A new video courseware - typhoon intensity forecasting - was incorporated into the training this time. It is a 5-class hour course consisting of the typhoon intensity forecasting, basic typhoon genesis and development conditions, typhoon intensity ensemble forecasting, and typhoon numerical model system.

2）Courseware Resources Newly Added to CMDEN

There are altogether 46.5 hours of typhoon-related courseware resources plus one 10-minute typhoon micro-lecture on CMDEN:

"Advanced Synoptics" Lecture 9:

Typhoon Structure, Genesis and Track	4 class hours
Typhoon Rainstorms and Severe Convection	10 class hours

"A Concise Course on Synoptics" Chapter 8:

Low Latitude Weather System (6)

Typhoon Formation Mechanism	5 class hours
Multi-Typhoons Interaction 1-2	2 class hours

QX/T 170-2012 Technical Practices for Typhoon Disaster Impact Assessment — 1 class hour

Typhoon Remote-Sensing Monitoring Methods and Latest Developments — 2 class hours

"Typhoon Forecast and Typhoon Disasters" — 22.5 class hours

Introduction to Typhoon
Tropical Weather Analysis
Typhoon Positioning Analysis
Typhoon Intensity Analysis
Typhoon Track Prediction
Typhoon Intensity Estimation
Typhoon Rainstorm Forecast
Typhoon Gale Forecast
(Approved recently, not yet displayed online)

By now, typhoon-related courseware has totaled 46.5 class hours.

From January to September 2020 the typhoon-related courseware has been studied by 759 learners for a total of 11,620 hours.

Contact Information: CMA Training Centre

Annexes

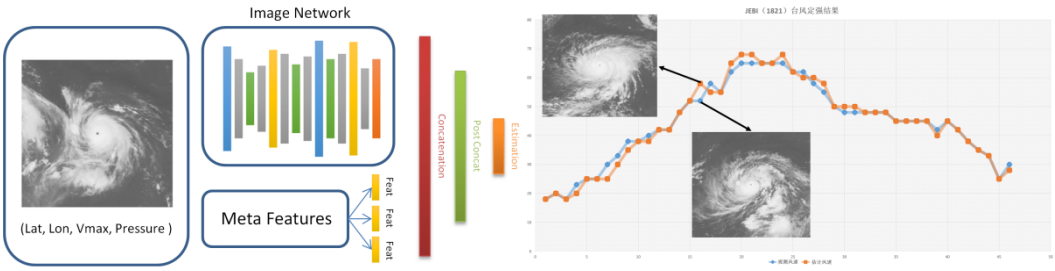

Fig. 2.1 Typhoon Intelligent Intensity Estimation System (TIIES) Technical Roadmap (a) and Result (b)

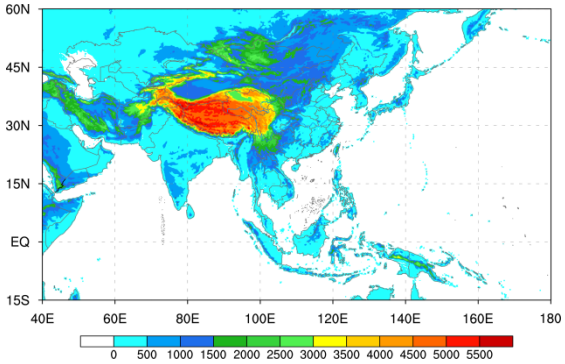

Fig. 2.2 GRAPES_TYM Forecast Coverage in 2020

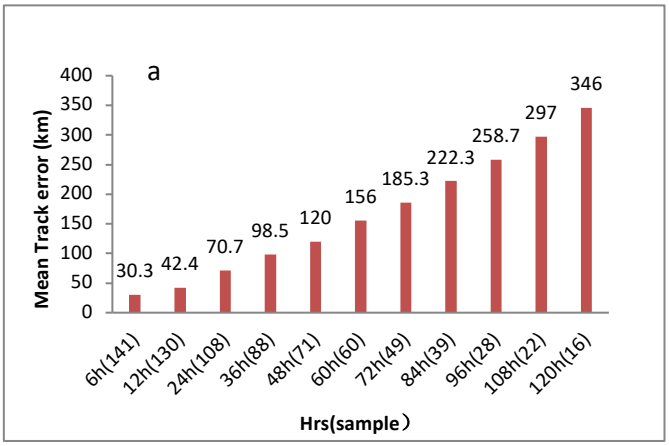

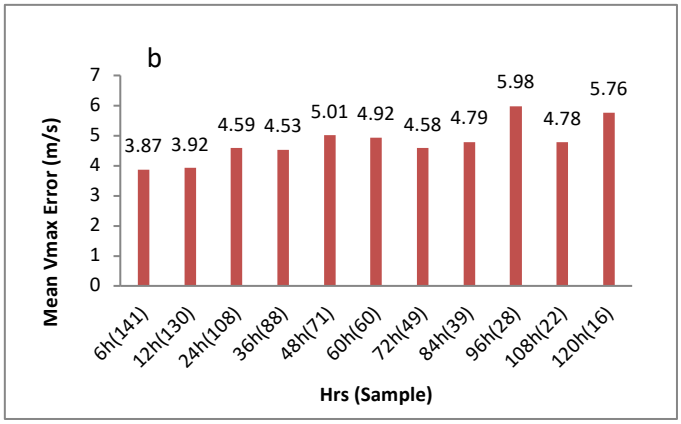

Fig.2.3 2020 GRAPES_TYM Average Forecat Error (a): Track Errors, (b): Intensity Errors

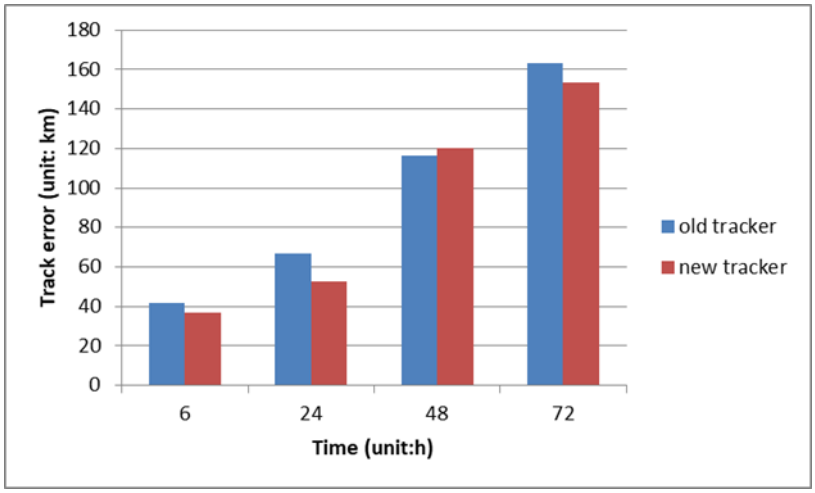

Fig.2.4 2020 TRAMSTyphoon Positioning Errors

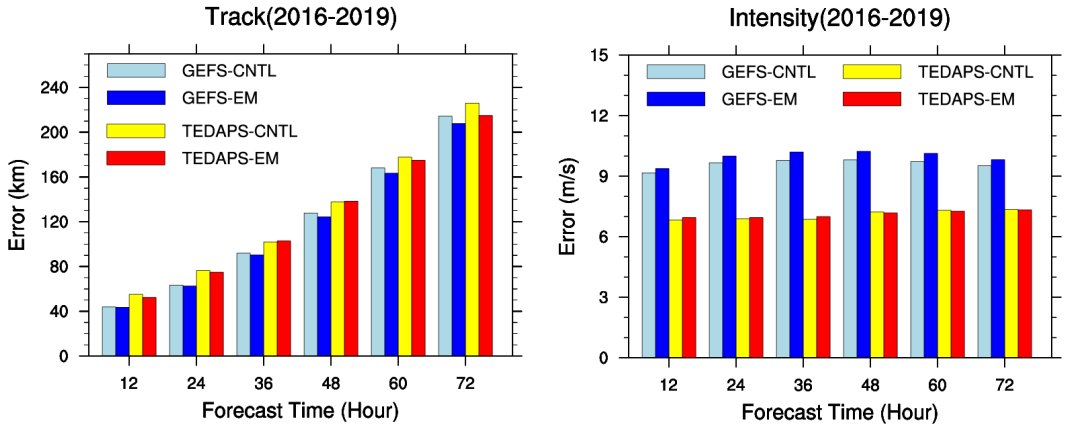

Fig.2.5 Comparison of 2016-2019 TEDAPS and NCEP-GEFS Errors

(Left: Track Erros; Right: Intensity Errors; CNTL, for Controlled Forcast; EM, for Ensemble Mean)

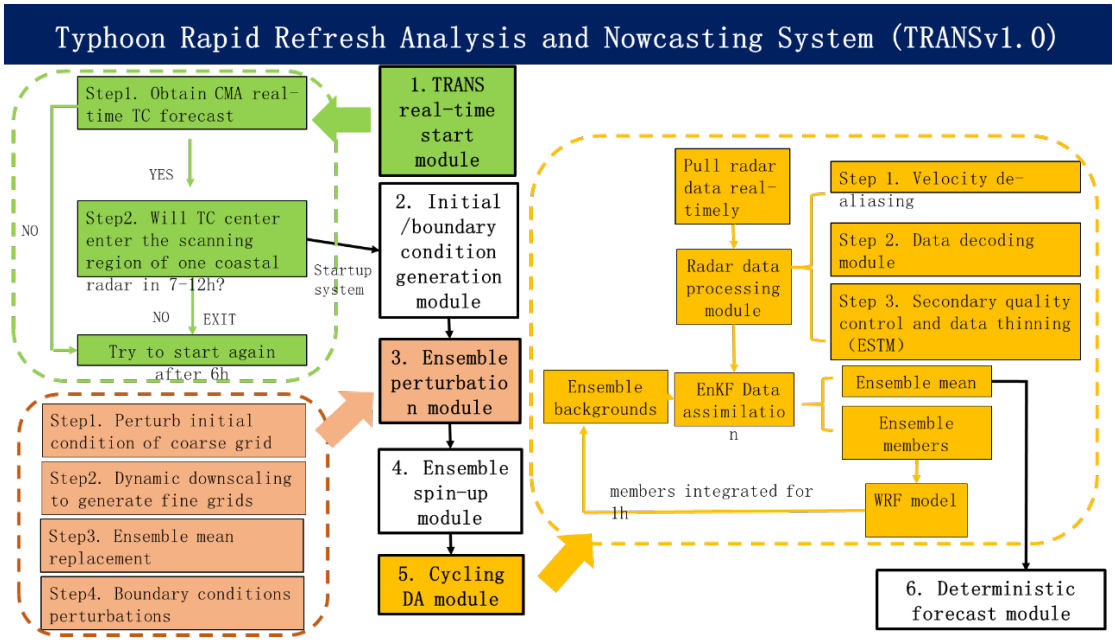

Fig.2.6 TRANSv1.0 Flow Chart

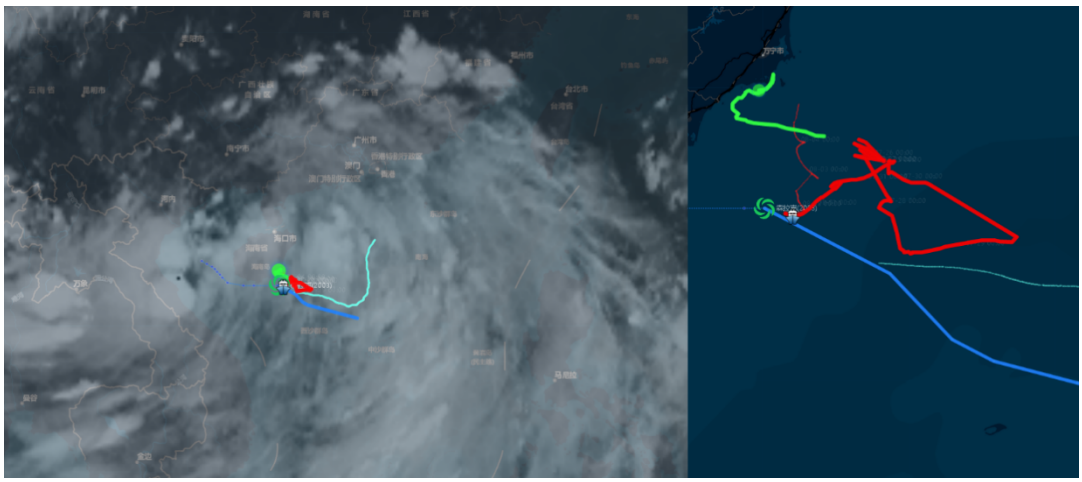

Fig.2.7 Illustration of the Positions of Buoys, Unmanned Boats, snd Typhoon Cloud System

during the Typhoon“Sinlaku” Observation Experiment

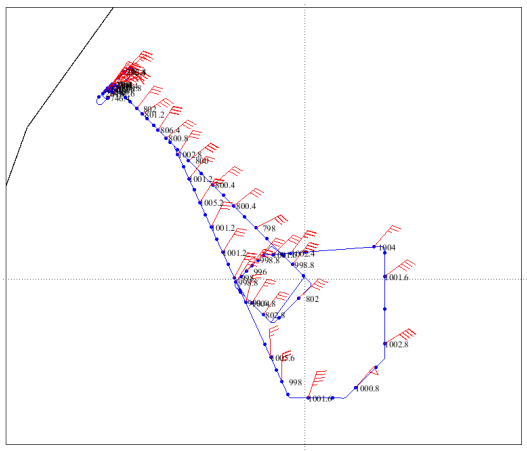

Fig.2.8 “Nangka” UAV Flight Route and Observation Altitude Vector Wind

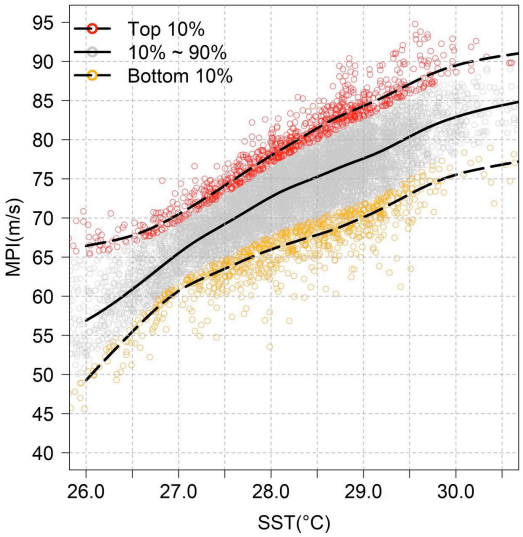

Fig.2.9 All Samples (All Dots), Top 10% (T10, Red Dot) and Bottom10% (B10, Yellow Dots)

TC-MPI Samples and Corresponding Medians: Black Solid Curves for All Samples; Upper Dashed Line for Top10%; Lower Dashed Line for Bottom10%)

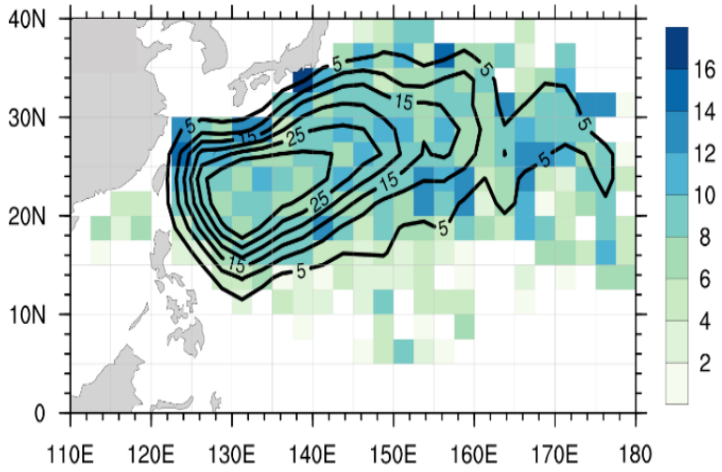

Fig.2.10 1980-2017 Typhoon-Season (June-November) Frquency of Typhoon Activities (Contour)

And Attenuation Rate in the 2.5°×2.5° Grid (Shaded, Unit: m/s/day)

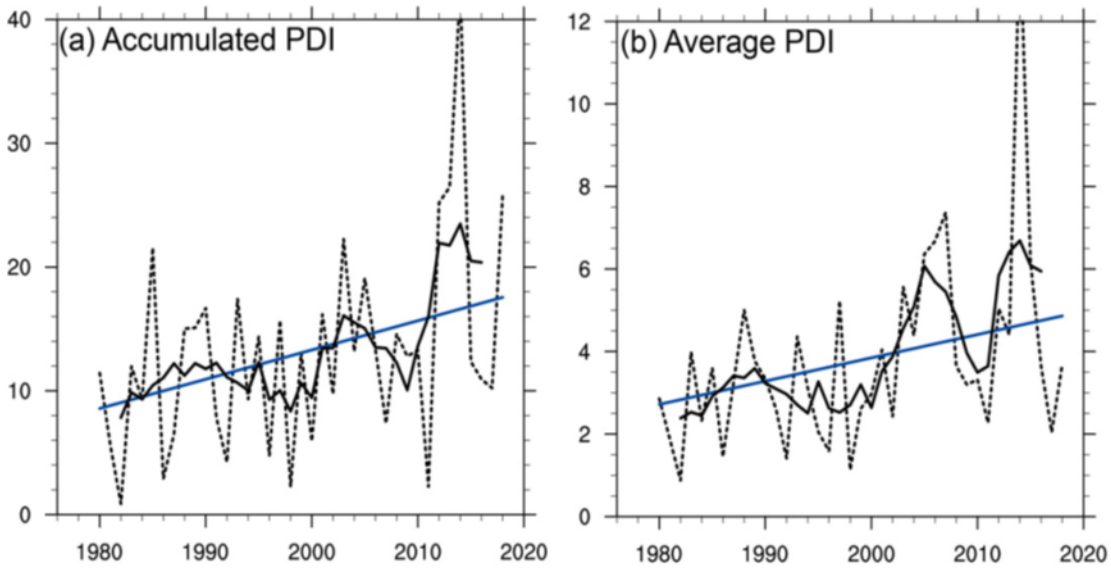

Fig.2.11 1980-2018 TC Landfalls in China (a) Accrued PDI, (b) Average PDI

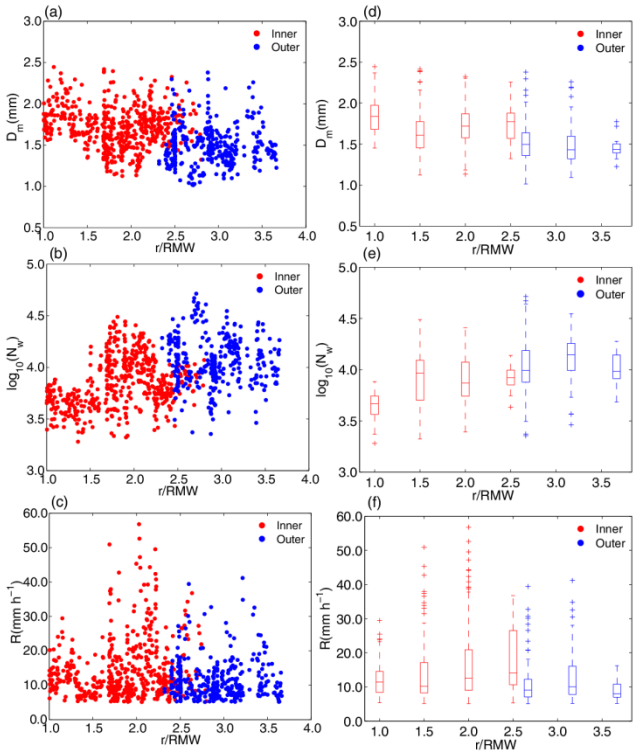

Fig.2.12 CIR (Red) and COR (Blue) (a) Mass-Weighted Diameter Dm (mm), (b) Normalized Intercept Parameter log10Nw (mm–1 m–3), and (c) Scatter Plot of Radius Distribution of Precipitation Rate (mm h–1), the abscissa normalized by the maximum wind speed radius (r/RMW). (d–f) Quartile Chart (Interval 0.5RMW)

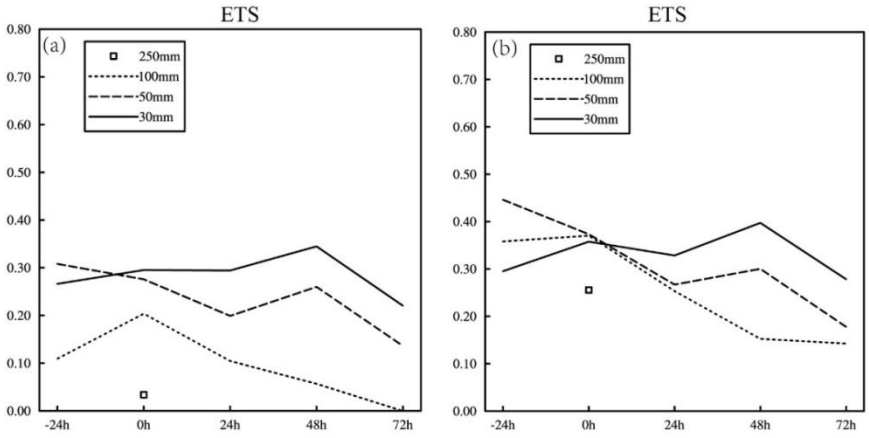

Fig.2.13 (a) ETS Scores of the Precipitation Forecast Verification Method at Different Stages of the Typhoon Life Cycle (weakened into a Depression 12h before landfall); (b) ETS Score of the CRA-Corrected Typhoon Precipitation Verification Indicators. Abiscissa-24/0/24/48/72h suggest 24h before landfall, during landfall and 24/48/72h after landfall; ordinate, ETS score. Solid line, 30mm; dashed line, 50mm; dotted line, 100mm; square, 250mm.

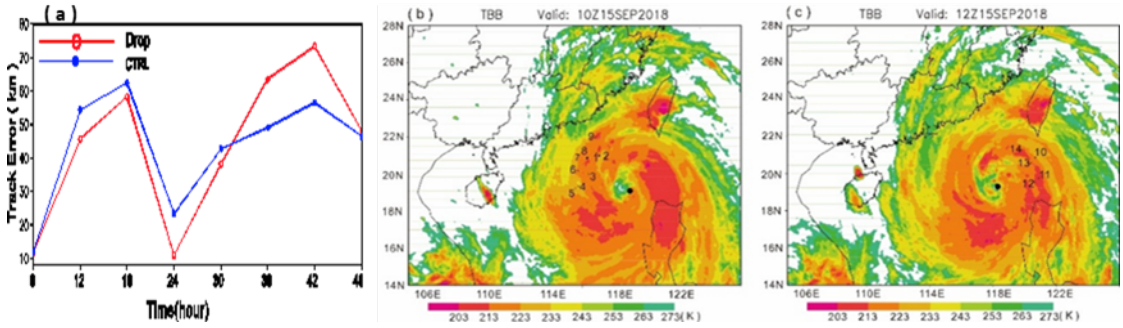

Fig.2.14 (a) Track Error after Dropsonde Data Assimilation, Red for Assimilation, Black for Controlled Experiment; Dropsonde Location and Blackbody Temperature (TBB) at (b) 1000UTC 15 Sept., 2018; (c) 1200UTC 15 Sept., 2018 . Black dot, Typhoon Center.

Fig. 2.15 Media Briefing on Renaming Yutu Entitled “Hi, Let Me Give It a Name”